

## ORIGIN AND DYNAMICAL SUPPORT OF IONIZED GAS IN GALAXY BULGES

LUIS C. HO

The Observatories of the Carnegie Institution of Washington, 813 Santa Barbara Street, Pasadena, CA 91101

*To appear in The Astrophysical Journal*

### ABSTRACT

We combine ionized gas ([N II]  $\lambda 6583$ ) and stellar central velocity dispersions for a sample of 345 galaxies, with and without active galactic nuclei (AGNs), to study the dynamical state of the nuclear gas and its physical origin. The gas dispersions strongly correlate with the stellar dispersions over the velocity range of  $\sigma \approx 30\text{--}350$  km s<sup>-1</sup>, such that  $\sigma_g/\sigma_* \approx 0.6\text{--}1.4$ , with an average value of 0.80. These results are independent of Hubble type (for galaxies from E to Sbc), presence or absence of a bar, or local galaxy environment. For galaxies of type Sc and later and that have  $\sigma_* \lesssim 40$  km s<sup>-1</sup>, the gas seems to have a minimum threshold of  $\sigma_g \approx 30$  km s<sup>-1</sup>, such that  $\sigma_g/\sigma_*$  always exceeds 1. Within the sample of AGNs,  $\sigma_g/\sigma_*$  increases with nuclear luminosity or Eddington ratio, a possible manifestation of AGN feedback associated with accretion disk winds or outflows. This extra source of nongravitational line broadening should be removed when trying to use  $\sigma_g$  to estimate  $\sigma_*$ . We show that the mass budget of the narrow-line region can be accounted for by mass loss from evolved stars. The kinematics of the gas, dominated by random motions, largely reflect the velocity field of the hot gas in the bulge. Lastly, we offer a simple explanation for the correlation between line width and line luminosity observed in the narrow-line region of AGNs.

*Subject headings:* galaxies: active — galaxies: bulges — galaxies: ISM — galaxies: kinematics and dynamics  
— galaxies: nuclei — galaxies: Seyfert

### 1. INTRODUCTION

Warm ( $\sim 10^4$  K), ionized gas is pervasive in the central regions of nearby galaxies of all morphological types. Easily detected through optical emission lines, either by imaging or spectroscopy, this component of the interstellar medium has served as a diagnostic of the physical conditions in galactic nuclei, including their source of excitation and chemical abundances. The optical line emission also provides a powerful tracer of the nuclear kinematics of the galaxy, in efforts to probe the mass distribution of the bulge, to detect central dark massive objects, and to study substructure such as kinematically decoupled cores.

What is the dynamical state of the nuclear gas? How does it relate to the dynamics of the stars? Is the gas primarily rotationally supported, or do random motions also contribute? While these issues have been addressed in the past, they have been based either on investigations of individual objects or small, restricted samples. A number of authors have noted, for example, that in the bulges of disk (lenticular and spiral) galaxies, the gas often rotates slower than the stars (Fillmore et al. 1986; Kent 1988; Kormendy & Westpfahl 1989; Bertola et al. 1995; Cinzano et al. 1999; Pignatelli et al. 2001). The same phenomenon has been found in some elliptical galaxies (e.g., Caldwell 1984; Caldwell et al. 1986). The physical origin for this effect, however, is not entirely clear. An interesting possibility is that the gas experiences nonnegligible pressure support (e.g., Kent 1988; Cinzano & van der Marel 1994; Bertola et al. 1995; Fisher 1997), an idea consistent with the detection of large central line widths in many bulge-dominated galaxies (e.g., Demoulin-Ulrich et al. 1984; Phillips et al. 1986; Bertola et al. 1995). Vega Beltrán et al. (2001) compiled gas and stellar velocity measurements for a sample of  $\sim 40$  disk galaxies to examine trends with Hubble type. They conclude that, with a few exceptions, the gas is dynamically cold, confined to a disk supported mainly by rotation.

What is the role of nongravitational forces on the gas dynamics, especially in objects harboring active galactic nuclei (AGNs)? This issue has been investigated most thoroughly in the context of the narrow-line region (NLR) in radio (Heckman et al. 1985; Smith et al. 1990; Baum & McCarthy 2000; Noell-Storr et al. 2007) and luminous Seyfert (e.g., Whittle 1992b, 1992c; Nelson & Whittle 1996) galaxies. The overall consensus from these studies is that the velocity field of the NLR gas largely traces the gravitational potential of the bulge of the host galaxy. Super-virial motions can be found, but only in the minority of objects exhibiting powerful, jetlike radio structures, which presumably impart additional mechanical acceleration to the gas. Comparing the widths of the optical nebular lines and the stellar velocity dispersions of a large sample of relatively luminous Seyfert 2 galaxies, Greene & Ho (2005a) reinforced the notion that the stellar potential principally governs the kinematics of the NLR, with important exceptions arising in cases where nuclear activity is especially strong. To date, much less attention has been paid to more garden-variety AGNs such as low-luminosity Seyferts and LINERs, or to nuclei powered by massive stars.

The Palomar spectroscopic survey of nearby galaxies (Ho et al. 1995, 1997a, and references therein) offers an excellent opportunity to examine some of the issues mentioned above. In addition to the existing extensive database of emission-line widths, a catalog of central stellar velocity dispersions is now available (Ho et al. 2009). This allows a detailed comparison of the central velocity dispersions of the gas and stars for a large, well-defined sample of galaxies spanning a wide range of Hubble types and nuclear spectral classes. This is the goal of this paper.

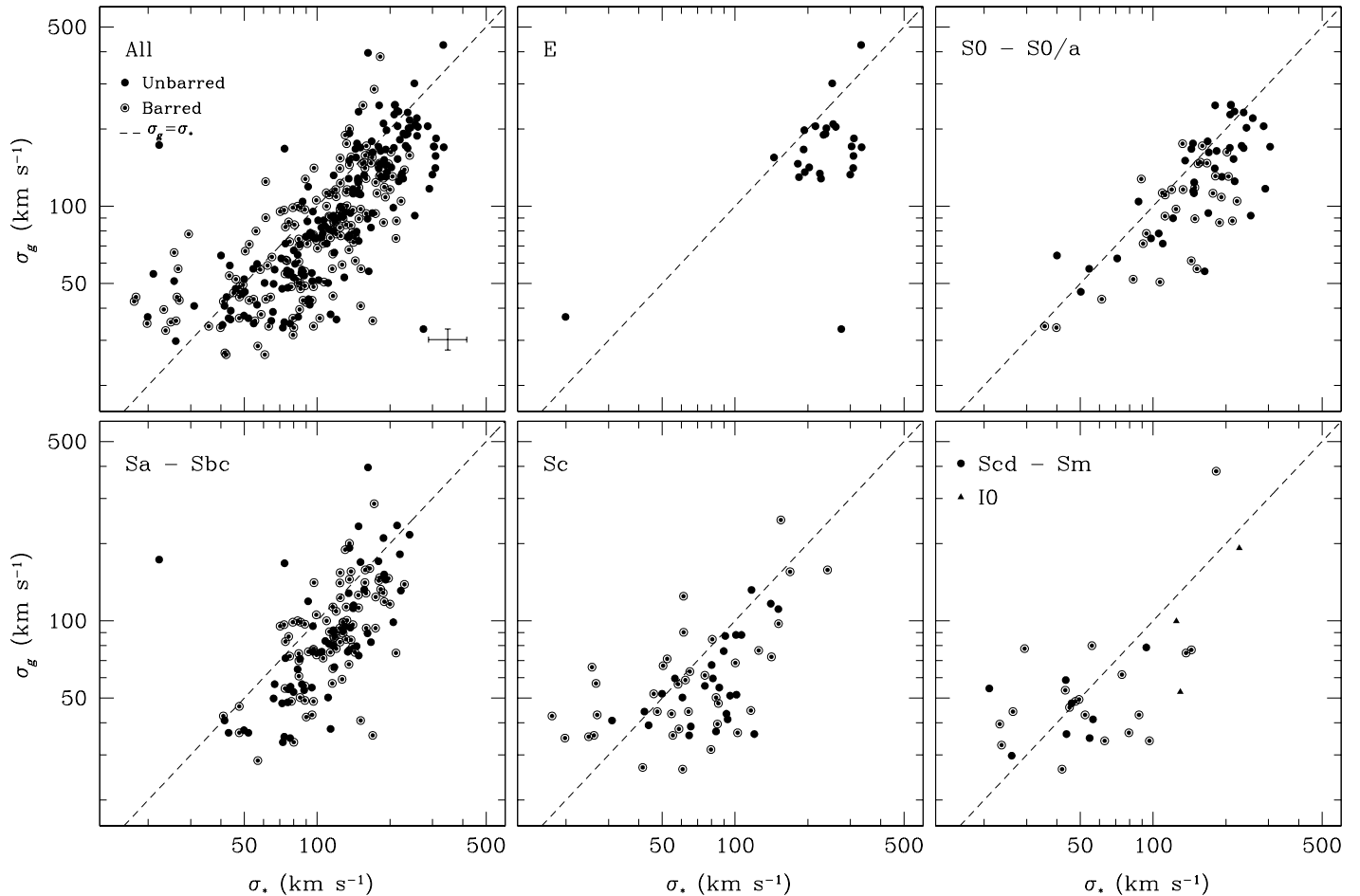


FIG. 1.— Distribution of gas ( $\sigma_g$ ) versus stellar ( $\sigma_*$ ) velocity dispersion as a function of Hubble type. Unbarred and barred galaxies are plotted as filled and encircled points, respectively. The dashed line denotes  $\sigma_g = \sigma_*$ . A typical error bar is given in the lower-right corner of the first panel.

## 2. SAMPLE AND DATA

Our analysis draws from the nearly complete, magnitude-limited sample of 486 bright galaxies spectroscopically surveyed using the Palomar 5-meter telescope. We focus on the galaxies that have well-measured widths (FWHM) for [N II]  $\lambda 6583$ , which, as explained in Ho et al. (1997a), is the line of choice in the Palomar survey for profile measurements. The majority of the Palomar galaxies (428/486 or 88%) now have central stellar velocity dispersion determined directly from the original survey data (Ho et al. 2009). Although many of the galaxies have preexisting velocity dispersion measurements in the literature, the Palomar data constitute a self-consistent, homogeneous set of measurements. A significant fraction of the galaxies (30%) have dispersions measured for the first time. Of the 407 galaxies that have FWHM([N II]) measurements, 372 (91%) have stellar velocity dispersions. If we confine our attention to the sources that have FWHM([N II]) measurements with a quality rating of “b” or better (see Ho et al. 1997a), excluding a handful of objects with only upper limits on their line widths, 345 have stellar velocity dispersions.

The above subset of 345 objects, the focus of this paper, rep-

resents fairly the parent population of emission-line nuclei in the Palomar survey. The 25 E, 70 S0–S0/a, 149 Sa–Sbc, 62 Sc, and 30 Scd–Sm galaxies constitute, respectively, 81%, 93%, 96%, 84%, and 48% of the parent population of emission-line objects. In terms of the nuclear spectral classes, the coverage is excellent for the AGNs: the present subsample contains 94% of the Seyferts, 93% of the LINERs, and 92% of the transition nuclei<sup>1</sup> in the parent survey. The high completeness fractions simply reflect the high AGN detection rate in bulge-dominated galaxies (Ho et al. 1997b), for which velocity dispersions are easier to obtain. By comparison, H II nuclei are 72% complete in the current sample—still a very high fraction.

## 3. THE CORRELATION BETWEEN $\sigma_g$ AND $\sigma_*$

### 3.1. Dependence on Hubble Type

Figure 1 shows the overall correlation between gas ( $\sigma_g$ ) and stellar ( $\sigma_*$ ) velocity dispersions, first for the entire sample, and then individually for several Hubble type bins. Most of the narrow emission lines, especially near the core, do not deviate strongly from a simple Gaussian (see Ho et al. 1997d), and we define  $\sigma_g \equiv \text{FWHM}([\text{N II}])/2.35$ . Barred galaxies, taken to be those designated as “SB” or “SAB” in the Third Reference Catalogue of Bright Galaxies (de Vaucouleurs et al. 1991), are

<sup>1</sup>See Ho et al. (1997a) for definition of the spectral classifications.

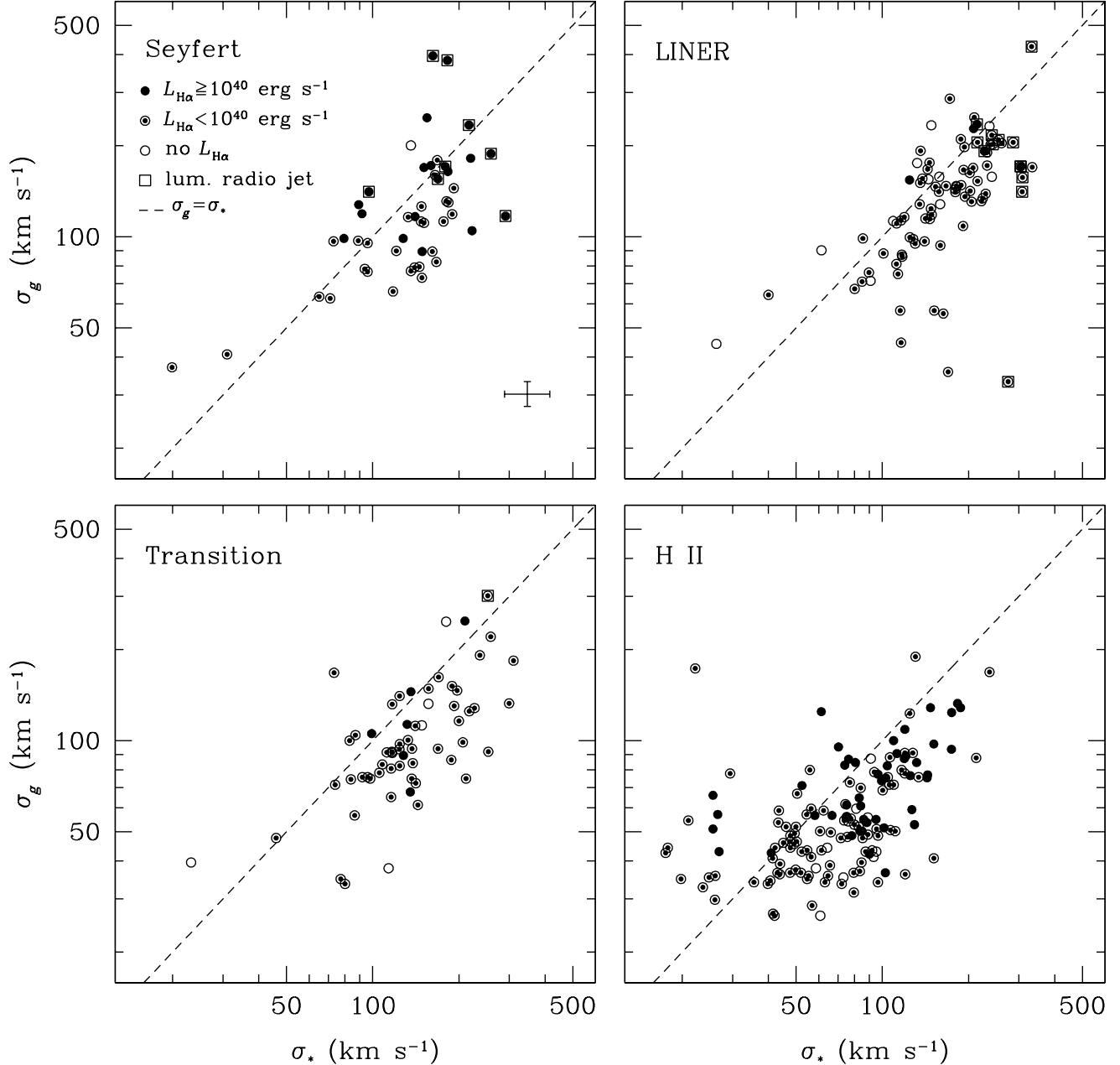


FIG. 2.— Distribution of gas ( $\sigma_g$ ) versus stellar ( $\sigma_*$ ) velocity dispersion as a function of nuclear spectral class. The symbols are coded according to H $\alpha$  luminosity. Objects containing linear radio sources with 6 cm powers greater than  $10^{21.7}$  W Hz<sup>-1</sup> are marked with boxes. The dashed line denotes  $\sigma_g = \sigma_*$ . A typical error bar is given in the lower-right corner of the first panel.

marked for emphasis. It is clear that  $\sigma_g$  correlates strongly with  $\sigma_*$ , albeit with considerable scatter. For the sample as a whole, the Kendall's  $\tau$  correlation coefficient (Isobe et al. 1986) is  $r = 1.19$ , which rejects the null hypothesis of no correlation with a probability of  $P_{\text{null}} < 10^{-4}$ . Both  $\sigma_g$  and  $\sigma_*$  cover approximately the same range<sup>2</sup> of velocities, from  $\sim 30$  to  $350$  km s<sup>-1</sup>. Although the correlation is most evident for the entire sample, the same trend replicates for the various Hubble type bins. It is least well-defined for the elliptical and extreme late-type (Scd–Sm and I0) galaxies because of the small sam-

ples and limited dynamic range in velocity dispersions. Thus, to first order, the gas velocities seem to track the random velocities of the stars. Quantitatively, however, the gas dispersions are systematically slightly *lower* than the stellar dispersions, on average by a constant offset of  $\sim 20\%$ . Defining the residuals from the  $\sigma_g = \sigma_*$  line by  $\Delta\sigma \equiv \log \sigma_g - \log \sigma_*$ ,  $\langle \Delta\sigma \rangle = -0.099 \pm 0.010$ . Barred and unbarred galaxies behave the same, with  $\langle \Delta\sigma \rangle = -0.094 \pm 0.014$  and  $-0.104 \pm 0.014$ , respectively. At the lowest velocities,  $\sigma_* \lesssim 40$  km s<sup>-1</sup>, nearly all the objects have  $\Delta\sigma > 0$ . This subgroup of high- $\Delta\sigma$  objects

<sup>2</sup>The lower limit of the velocities, however, is strongly influenced by the spectral resolution of the Palomar survey, which is  $\sigma \approx 40$  km s<sup>-1</sup> in the red and  $\sim 120$  km s<sup>-1</sup> in the blue (Ho et al. 1997a). Published stellar velocity dispersions often are also not very reliable for low-dispersion galaxies. Thus, we consider the region defined by  $\sigma_g \lesssim 40$  km s<sup>-1</sup> and  $\sigma_* \lesssim 40$  km s<sup>-1</sup> to be quite uncertain.

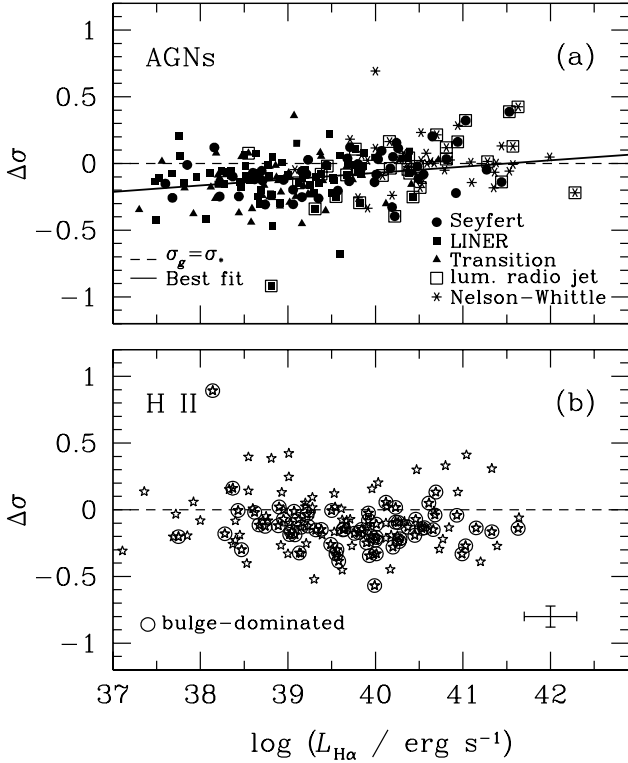


FIG. 3.— Residuals of the  $\sigma_g$ - $\sigma_*$  correlation,  $\Delta\sigma \equiv \log \sigma_g - \log \sigma_*$ , as a function of  $H\alpha$  luminosity  $L_{H\alpha}$ , for (a) all AGNs (Seyferts, LINERs, and transition objects), including the sample of luminous Seyferts from Nelson & Whittle (1995), and (b) H II nuclei. Objects with linear radio sources and  $P_{6\text{cm}} > 10^{21.7} \text{ W Hz}^{-1}$  are marked with boxes. The dashed line denotes  $\sigma_g = \sigma_*$ . The solid line in panel (a) shows the best-fit regression line. A typical error bar is given in the lower-right corner of the panel (b).

cannot be attributed entirely to resolution effects because only a small number of [N II] profiles are unresolved and including them does not alter the distribution of data points. Rather, it appears that galaxy centers reach a “floor” at  $\sigma_g \approx 30 \text{ km s}^{-1}$ .

In detail, the different Hubble types also have similar distributions:  $\langle \Delta\sigma \rangle = -0.15 \pm 0.043$ ,  $-0.105 \pm 0.018$ ,  $-0.113 \pm 0.014$ , and  $-0.083 \pm 0.026$  for E, S0–S0/a, Sa–Sbc, and Sc, respectively. Ellipticals appear to have somewhat larger offsets than the disk galaxies, but the means of the different samples are not statistically different according to the Student’s  $t$  test. By contrast, very late-type objects, in our sample dominated by Scd–Sm galaxies, clearly stand apart with  $\langle \Delta\sigma \rangle = -0.036 \pm 0.041$ , differing mildly from the other groups at a significance of 94%.

### 3.2. Dependence on Local Environment

Ho et al. (1997a) give two parameters to gauge the tidal influence of nearby neighbors: (1)  $\rho_{\text{gal}}$ , the density of galaxies brighter than  $M_B = -16$  mag in the object’s local vicinity, and (2)  $\theta_p$ , the projected angular separation to the nearest neighbor within a magnitude difference of  $\pm 1.5$  mag and a velocity difference of  $\pm 500 \text{ km s}^{-1}$ . We find that  $\Delta\sigma$  shows no correlation with either  $\rho_{\text{gal}}$  or  $\theta_p$ .

### 3.3. Dependence on AGN Properties

We next evaluate the dependence of the  $\sigma_g$ - $\sigma_*$  correlation on nuclear spectral classification (Fig. 2). The four classes

of emission-line objects appear broadly similar, but in detail there are some subtle, important differences. Taken at face value, the Seyfert sample shows the least degree of offset from the  $\sigma_g = \sigma_*$  line. Its distribution of  $\Delta\sigma$ , with an average value of  $-0.054 \pm 0.025$ , statistically differs from that of transition nuclei ( $\langle \Delta\sigma \rangle = -0.13 \pm 0.021$ ) at a significance level of 98% according to the Student’s  $t$  test. LINERs, with  $\langle \Delta\sigma \rangle = -0.095 \pm 0.019$ , lie sandwiched in between, although formally the differences are only statistically marginal. Combining all three AGN subclasses,  $\langle \Delta\sigma \rangle = -0.096 \pm 0.012$ .

As a group, H II nuclei have an overall  $\langle \Delta\sigma \rangle = -0.103 \pm 0.017$ . However, as mentioned in § 3.1, late-type spirals, which largely dominate the H II class, seem to comprise two distinct populations divided roughly at  $\sigma_* \approx 40 \text{ km s}^{-1}$ . Below this value, our sample of H II nuclei has  $\langle \Delta\sigma \rangle = +0.28 \pm 0.055$ ; above it,  $\langle \Delta\sigma \rangle = -0.15 \pm 0.013$ .

Whittle (1992b, 1992c) and Nelson & Whittle (1996) suggested that Seyfert galaxies with radio sources that are both strong and linearly extended tend to have emission lines that are systematically broader than the stellar velocities. They interpret this to mean that the outflowing radio jets provide a secondary, nongravitational source of acceleration to the NLR gas. Whittle (1992b, 1992c) chose  $P_{20\text{cm}} = 10^{22.5} \text{ W Hz}^{-1}$  as the threshold between strong and weak radio sources. We have adopted this criterion<sup>3</sup>, and with the radio data for the Palomar low-luminosity AGNs presented in Ho & Ulvestad (2001) and elsewhere (Ho 2008, and references therein), highlighted in Figure 2 the objects with luminous, jetlike radio sources. Two of the objects in this subset—NGC 1068 and NGC 3079—are clearly systematically offset above the rest. But another six that satisfy the same radio criteria do not look extraordinary whatsoever, and not all high- $\Delta\sigma$  objects have strong radio jets. The same trends hold for luminous radio sources among the LINERs and transition objects. As a whole, strong radio jets are neither necessary nor sufficient to produce super-virial velocities in the NLR.

Closer inspection of Figure 2 reveals a more interesting effect within the AGN samples. When the objects are flagged according to  $H\alpha$  luminosity, those with high luminosities—here, for illustrative purposes, chosen somewhat arbitrarily to be those above  $L_{H\alpha} = 10^{40} \text{ erg s}^{-1}$ —tend to lie systematically displaced toward higher  $\Delta\sigma$  compared to objects with lower luminosities. (We use the narrow component of the  $H\alpha$  luminosity, corrected for Galactic and internal extinction.) This is most clearly seen for the Seyfert sample. It is less obvious for the LINERs and transition objects because of the paucity of luminous sources in these classes (Ho et al. 2003), but the same trend is noticeable nonetheless. Within the Seyfert sample,  $\langle \Delta\sigma \rangle = +0.004 \pm 0.043$  for objects with  $L_{H\alpha} \geq 10^{40} \text{ erg s}^{-1}$  and  $\langle \Delta\sigma \rangle = -0.10 \pm 0.026$  for objects with  $L_{H\alpha} < 10^{40} \text{ erg s}^{-1}$ . The difference between the two means is significant at the level of 96%.

To explore the luminosity effect further, we augmented the Palomar sample with 52 Seyfert nuclei from the work of Nelson & Whittle (1995) that were not already in the Palomar survey. These additional objects provide better coverage at the high-luminosity end.  $H\alpha$  luminosities were converted from  $H\beta$  luminosities given in Nelson & Whittle (1995) and Whittle (1992a), assuming  $H\alpha/H\beta = 3.1$  (Gaskell & Ferland 1984) and adjusted to a Hubble constant of  $H_0 = 75 \text{ km s}^{-1} \text{ Mpc}^{-1}$ . Figure 3a plots  $\Delta\sigma$  against  $L_{H\alpha}$  for the combined sample of AGNs, again flagging the luminous, extended radio sources. Note the nonzero

<sup>3</sup>Whittle (1992b, 1992c) assumes a Hubble constant of  $H_0 = 50 \text{ km s}^{-1} \text{ Mpc}^{-1}$  and a reference wavelength of 20 cm, whereas we use  $H_0 = 75 \text{ km s}^{-1} \text{ Mpc}^{-1}$  and a reference wavelength of 6 cm. The corresponding threshold, for a spectrum  $f_\nu \propto \nu^{-0.7}$ , is  $P_{6\text{cm}} = 10^{21.7} \text{ W Hz}^{-1}$ .

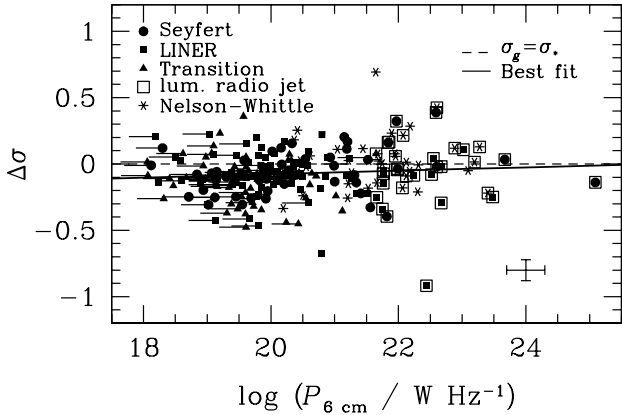


FIG. 4.— Residuals of the  $\sigma_g$ - $\sigma_*$  correlation for the AGNs (Seyferts, LINERs, and transition objects in the Palomar survey, plus the luminous Seyferts from Nelson & Whittle 1995),  $\Delta\sigma$ , as a function of  $P_{6\text{cm}}$ , the 6 cm power. The symbols for the different sources are given in the figure legend. Objects with linear radio sources and  $P_{6\text{cm}} > 10^{21.7}$  W Hz $^{-1}$  are marked with boxes. The dashed line denotes  $\sigma_g = \sigma_*$ . The solid line gives the best-fit regression line. A typical error bar is shown in the lower-right corner.

slope. A correlation can be seen for the Seyferts alone, as well as for the combined sample of LINERs and transition nuclei. Treating  $\log L_{\text{H}\alpha}$  as the independent variable, an ordinary least-squares regression fit to all the points gives

$$\Delta\sigma = (0.047 \pm 0.015) \log L_{\text{H}\alpha} - (1.95 \pm 0.59), \quad (1)$$

with an rms scatter of 0.17 dex. The scatter reduces to 0.16 dex with the luminous radio sources excluded. The correlation has high statistical significance: the generalized Kendall's  $\tau$  test yields  $r = 0.47$  and  $P_{\text{null}} < 10^{-4}$ . Omitting the flagged radio sources has little effect on the results. By contrast, the sample of H II nuclei (Fig. 3b) does *not* show this effect, even though the H II nuclei and AGNs span essentially the same range in H $\alpha$  luminosities. The different behavior of H II nuclei compared to AGNs cannot be attributed to differences in morphological types. Roughly half of the H II nuclei are hosted in bulge-dominated (S0–Sbc;  $T = -2$  to 4) galaxies, and these follow the same pattern as the rest of the sample (Fig. 3b).

In Figure 4, we substitute the H $\alpha$  luminosity with the 6 cm radio power. Radio data for the Palomar Seyferts come from Ho & Ulvestad (2001), and those for the supplementary sample of luminous objects come from Nelson & Whittle (1995) and Whittle (1992a). Data for the LINERs and transition objects are taken from a variety of sources, as summarized in Ho (2008). Again, we see a positive, significant trend, although formally it is weaker than that for  $L_{\text{H}\alpha}$ . In this case the Kendall's  $\tau$  correlation coefficient is  $r = 0.29$ , with  $P_{\text{null}} = 6 \times 10^{-4}$ . A linear regression fit, calculated using the method of Schmitt (1985), which properly treats the few censored radio data points, gives

$$\Delta\sigma = (0.013 \pm 0.0085) \log P_{6\text{cm}} - (0.34 \pm 0.17). \quad (2)$$

The tendency for  $\Delta\sigma$  to increase with optical and radio power suggests that the AGN luminosity, over a wide range of values, injects an additional, systematic contribution to the line broadening.

Lastly, Figure 5 illustrates that an even stronger correlation exists between  $\Delta\sigma$  and the Eddington ratio, which is proportional to the mass accretion rate. As in Greene & Ho (2007), we estimate the bolometric luminosity from the H $\alpha$  luminosity, converting  $L_{\text{H}\alpha}$  to  $L_{5100}$  using the line-continuum correlation of Greene & Ho (2005b) and then adopting  $L_{\text{bol}} = 9L_{5100}$ .

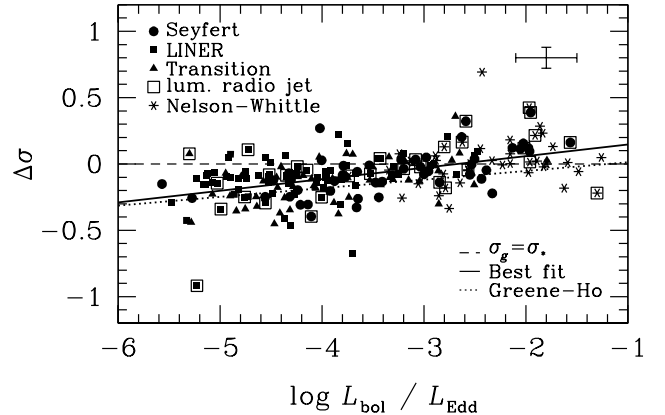


FIG. 5.— Residuals of the  $\sigma_g$ - $\sigma_*$  correlation for the AGNs (Seyferts, LINERs, and transition objects in the Palomar survey, plus the luminous Seyferts from Nelson & Whittle 1995),  $\Delta\sigma$ , as a function of Eddington ratio,  $L_{\text{bol}}/L_{\text{Edd}}$ . The symbols for the different sources are given in the figure legend. Objects with linear radio sources and  $P_{6\text{cm}} > 10^{21.7}$  W Hz $^{-1}$  are marked with boxes. The dashed line denotes  $\sigma_g = \sigma_*$ . The solid line gives the best-fit regression line; the dotted line shows the relation found by Greene & Ho (2005a; Equation 4). A typical error bar is shown in the upper-right corner.

We use the  $M_{\text{BH}} - \sigma_*$  relation of Tremaine et al. (2002) to obtain the black hole mass and hence the Eddington luminosity,  $L_{\text{Edd}} = 1.26 \times 10^{38} (M_{\text{BH}}/M_{\odot})$  erg s $^{-1}$ . The Kendall's  $\tau$  correlation coefficient now rises to  $r = 0.74$ , with  $P_{\text{null}} < 10^{-4}$ . An ordinary least-squares regression fit with  $\log L_{\text{bol}}/L_{\text{Edd}}$  as the independent variable gives

$$\Delta\sigma = (0.087 \pm 0.011) \log L_{\text{bol}}/L_{\text{Edd}} + (0.23 \pm 0.042). \quad (3)$$

The correlation is surprisingly tight, with an rms scatter of only 0.15 dex. If we omit the sources with luminous radio jets, the scatter reduces even further to 0.14 dex.  $\Delta\sigma$  seems to correlate somewhat better with  $L_{\text{bol}}/L_{\text{Edd}}$  than with  $L_{\text{H}\alpha}$ , although formally, according to the  $t$  and  $F$  tests, neither the mean nor the variance of the residuals about the best-fit lines differs at a statistically significant level.

### 3.4. Geometry and Kinematics of the Ionized Gas

The gas line widths presented in this study were extracted from a single  $2'' \times 4''$  aperture centered on the nucleus, which corresponds to a region 200 pc  $\times$  400 pc for a typical distance of 20 Mpc (Ho et al. 1997a). Without spatially resolved data, it is impossible to know a priori in any individual object whether the line width represents true velocity dispersion or instead arises from spatial smearing of a steep inner rotational gradient. Nevertheless, we can appeal to general arguments to test the scenario of rotational broadening. If the nuclear gas is confined to a rotating disk aligned with the large-scale galactic plane, one might naively expect the line width to correlate with the galaxy inclination angle. This effect is not seen in the Palomar survey (Ho 1996; Ho et al. 2003). However, as discussed by Whittle (1992b), this simple test is likely to be inconclusive because the line widths are primarily governed by virial velocities and AGN properties rather than by projection effects.

Instead, Whittle (1992b), as did Heckman et al. (1989), examined the correlation between inclination angle and the ratio  $\Delta V_{\text{rot}}/\text{FWHM}$ , where  $\Delta V_{\text{rot}}$  is the observed rotation amplitude of the large-scale disk and FWHM is the full-width at half maximum of the central line profile. If the central nebular emission

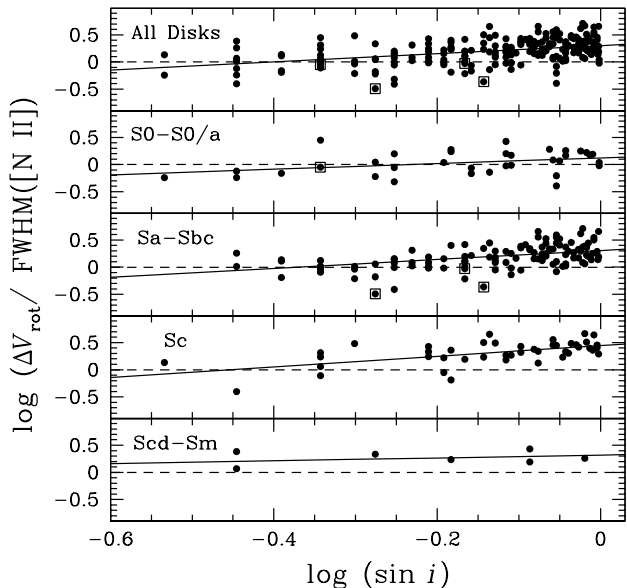


FIG. 6.— Distribution of the ratio  $\Delta V_{\text{rot}}/\text{FWHM}([\text{N II}])$  versus  $\sin i$  as a function of Hubble type. The dashed line denotes an idealized model wherein  $\text{FWHM}([\text{N II}])$  arises entirely from rotation in the galactic plane. Actual fits to the data, after excluding the luminous, linear radio sources (marked with squares), are given as solid lines; the regressions are calculated using an ordinary least-squares fit with  $\log \sin i$  as the independent variable.

arises from a coplanar nuclear disk,  $\text{FWHM}$ , like  $\Delta V_{\text{rot}}$ , is a projected quantity, and  $\Delta V_{\text{rot}}/\text{FWHM}$  will be independent of inclination. In the extreme alternative scenario where  $\text{FWHM}$  represents purely random velocity dispersion,  $\Delta V_{\text{rot}}/\text{FWHM}$  should correlate positively with inclination. The results of this exercise are shown in Figure 6 for all the non-elliptical galaxies, using data for  $\Delta V_{\text{rot}}$  (derived from integrated H I line widths) and inclination angle  $i$  from Ho et al. (1997a). In each panel, the coplanar rotation model is marked with the horizontal dashed line. The actual regression fit to the data (after excluding the flagged radio sources) is shown as a solid line. With the exception of the small number of very late-type (Scd–Sm) spirals, the vast majority of the sample strongly disagree with the coplanar rotation model.

As a final check, we also plotted the residuals  $\Delta\sigma$  from Figure 1 against  $\sin i$ . We find no correlation, as to be expected if  $\sigma_g$  and  $\sigma_*$  are both inclination-independent.

#### 4. DISCUSSION

##### 4.1. Estimating $\sigma_*$ from $\sigma_g$

We combine new central stellar velocity dispersions (Ho et al. 2009) with published emission-line width measurements (Ho et al. 1997a) to examine the relationship between the kinematics of the ionized gas and stars in the central regions of galaxies. Unlike most studies that primarily focus on the [O III]  $\lambda 5007$  line, ours uses [N II]  $\lambda 6583$ , which offers at least two major advantages. [N II] has a lower ionization potential and a lower critical density than [O III], making it a better tracer over a larger radial extent of the bulge. [N II] also provides a more reliable probe of the gravitational potential because it is less susceptible to contamination by outflows or other radial motions.

Like most narrow emission lines in AGNs, [N II] does exhibit line asymmetries indicative of radial flows (Ho 1996; Ho et al. 2003), but they seem to be less prevalent than in high-ionization transitions such as [O III] (Heckman et al. 1981; Vrtilik & Carleton 1985; Whittle 1985). Studies of AGN line profiles that include transitions from a wide range of ionization states (Busko & Steiner 1992; Greene & Ho 2005a) find that [S II]  $\lambda\lambda 6716, 6731$  generally tend to be less asymmetric than [O III] (but see Rice et al. 2006). Since the profile of [S II] empirically matches well the profile of [N II] (e.g., Ho et al. 1997d), it follows that [N II] is also less asymmetric than [O III]. Moreover, the average line centroid of [N II] is consistent with the systemic velocity of the host galaxy, whereas high-ionization lines such as [O III] are often blueshifted (Boroson 2005). Previous work that makes use of [N II] to probe the kinematics of the NLR include those of Phillips et al. (1986), Verdoes Kleijn et al. (2006), Zhou et al. (2006), Chen et al. (2008), and Walsh et al. (2008).

Our principal finding is that, within the central few hundred parsecs of galaxy bulges, the velocity dispersion of the ionized gas is comparable to, but typically somewhat lower than, the velocity dispersion of the stars. The rough correspondence between  $\sigma_g$  and  $\sigma_*$  indicates that the NLR is in dynamical equilibrium with the stellar potential. Defining  $\Delta\sigma = \log \sigma_g - \log \sigma_*$ ,  $\Delta\sigma$  ranges from  $-0.15$  to  $+0.08$ , with an average value of  $-0.099$ , or  $\langle \sigma_g/\sigma_* \rangle = 0.80$ . In detail,  $\Delta\sigma$  shows, at best, a mild variation with galaxy morphology but no discernible dependence on the presence of a large-scale bar or local galaxy environment. By contrast, the more luminous AGNs studied by Whittle (1992b) seem to exhibit broader lines in barred and interacting galaxies.

As an aside, we note that the late-type spirals in our sample show an intriguing property: below  $\sigma_* \approx 40 \text{ km s}^{-1}$ ,  $\Delta\sigma$  is *always* positive. It seems that in these late-type galaxies with small bulges (possibly all “pseudo-bulges”; Kormendy & Kennicutt 2004), the velocity dispersion of the warm ( $\sim 10^4 \text{ K}$ ) ionized gas has a floor of  $\sim 30 \text{ km s}^{-1}$ . This might represent a minimum threshold of interstellar turbulence in the central regions of present-day disk-dominated galaxies, maintained, perhaps, through stellar feedback associated with their modest star formation rates (Ho et al. 1997c). The dispersion threshold we find is qualitatively similar to the magnitude of non-ordered motions detected in the central regions of low-surface brightness galaxies (e.g., Kuzio de Naray et al. 2008; Pizzella et al. 2008a, 2008b).

The availability of a uniform set of nuclear spectroscopic classifications for the Palomar galaxies has prompted us to re-examine the kinematics of the NLR, their relationship with the stellar potential of the bulge of the host galaxy, and the possible role of nongravitational perturbations by AGNs. Previous treatment of this subject has concentrated almost exclusively on radio galaxies (Smith et al. 1990; Verdoes Kleijn et al. 2006; Noel-Storr et al. 2007) and relatively luminous Seyfert nuclei (Véron 1981; Terlevich et al. 1990; Veilleux 1991; Whittle 1992b, 1992c; Nelson & Whittle 1996; Jiménez-Benito et al. 2000; Botte et al. 2005; Greene & Ho 2005a; Bian et al. 2006; Zhou et al. 2006; Chen et al. 2008; Dasyra et al. 2008). The reviews by Wilson & Heckman (1985) and Whittle (1993) included some preliminary results on LINERs, although they were based on rather fragmentary data. They concluded that the NLR kinematics of LINERs, as in Seyferts, are largely virial. In their survey of ionized gas in E and S0 galaxies, most of which contain LINER nuclei, Phillips et al. (1986) compared

the FWHM of [N II]  $\lambda 6583$  with the absolute magnitude of the host galaxies and inferred that in general  $\sigma_g \lesssim \sigma_*$ .

Our analysis strongly reinforces the notion that gravity dominates the kinematics of the NLR, not only in Seyferts, but indeed in *all* emission-line nuclei found in nearby galaxies, including low-ionization, low-luminosity AGNs such as LINERs and transition objects, and even H II nuclei. The gas velocity dispersions are comparable to, but typically somewhat less than, the stellar velocity dispersions measured over a physical scale of typically 200–400 pc. The velocity discrepancy observed in H II nuclei and AGNs is about the same,  $\langle \sigma_g/\sigma_* \rangle \approx 0.8$ , with a surprisingly small standard deviation of only  $\sim 0.2$  dex. As in the work of Whittle (1992b, 1992c) and Nelson & Whittle (1996), we find that powerful radio jets, in the minority of nearby sources where they are found, do sometimes seem to exert secondary, super-virial acceleration on the NLR gas, although the correspondence is hardly one-to-one. However, the main new insight obtained from our work is that the impact of the central AGN may be more widespread and systemic than previously suspected. We find that, not only among Seyfert galaxies but also in the characteristically less powerful LINERs and transition nuclei, the offset between  $\sigma_g$  and  $\sigma_*$  varies mildly but *systematically* with the level of AGN activity. The effect can be seen with nuclear activity as gauged through optical (H $\alpha$ ) luminosity (Fig. 3a), radio luminosity (Fig. 4), and especially Eddington ratio (Fig. 5). The weakest AGNs in the Palomar sample (LINERs and transition nuclei with  $L_{\text{H}\alpha} \approx 3 \times 10^{37}$  erg s $^{-1}$ ,  $P_{6\text{cm}} \lesssim 10^{18}$  W Hz $^{-1}$ , and  $L_{\text{bol}}/L_{\text{Edd}} \approx 3 \times 10^{-6}$ ) are characterized by  $\sigma_g/\sigma_* \approx 0.6$ –0.8, while luminous sources (Seyferts with  $L_{\text{H}\alpha} \approx 3 \times 10^{41}$  erg s $^{-1}$ ,  $P_{6\text{cm}} \approx 10^{23}$  W Hz $^{-1}$ , and  $L_{\text{bol}}/L_{\text{Edd}} \approx 4 \times 10^{-2}$ ) can attain  $\sigma_g/\sigma_* \approx 1.2$ –1.4. Remarkably, H II nuclei, even those spanning a similar range in H $\alpha$  luminosity and Hubble type as the AGNs, do *not* follow these trends (Fig. 3b). Evidently the physical nature of the activity—stellar or nonstellar—matters.

It is worth noting that Whittle (1992b, 1992c) and Nelson & Whittle (1996) find  $\langle \sigma_g/\sigma_* \rangle \approx 0.9$  for their sample of Seyferts (after excluding the luminous, jetlike radio sources), somewhat larger than the average value of  $\langle \sigma_g/\sigma_* \rangle \approx 0.8$  for the Palomar objects. This difference is easy to explain in view of the luminosity dependence just mentioned, since Whittle’s sample is more luminous than the Palomar objects. In their analysis of emission-line objects from the Sloan Digital Sky Survey (SDSS), Chen et al. (2008) find, as we do in this study, that  $\sigma_g/\sigma_*$  varies slightly but systematically with nuclear spectral classification: transition objects have the lowest values and Seyferts the highest, with LINERs in between. This trend reflects none other than the dependence of  $\sigma_g/\sigma_*$  on luminosity or Eddington ratio. Ho (2008, 2009) proposes that the mass accretion rate, which scales with the Eddington ratio, is the primary physical driver responsible for variations in spectral classification. The accretion rate increases systematically along the sequence transition objects  $\rightarrow$  LINERs  $\rightarrow$  Seyferts.

If the size of the NLR scales with luminosity, Laor (2003) suggests that the NLR in low-luminosity AGNs may be sufficiently compact that its kinematics may be influenced more by the gravitational potential of the central black hole than by that of the surrounding bulge. Spatially resolved observations of the NLR in some LINERs at *Hubble Space Telescope* resolution indeed do find that the line widths are largest interior to the black hole’s gravitational sphere of influence, gradually merging at larger radii with the stellar dispersion of the bulge (Walsh et al.

2008). If this effect were dominant, however,  $\sigma_g/\sigma_*$  would rise with decreasing luminosity, exactly the opposite of what is seen in our sample. Evidently on a scale of several hundred parsecs the integrated kinematics of the NLR are controlled primarily by the gravitational potential of the stars and by AGN feedback.

The discovery of a tight relation between central black hole mass and bulge stellar velocity dispersion (the  $M_{\text{BH}}\text{-}\sigma_*$  relation: Gebhardt et al. 2000; Ferrarese & Merritt 2000) has prompted renewed interest in efficient methods to estimate  $\sigma_*$ , especially in objects such as luminous AGNs where this parameter is challenging to measure directly (Greene & Ho 2006). In view of the approximate equality between  $\sigma_g$  and  $\sigma_*$  and the ease with which [O III]  $\lambda 5007$  can be detected in AGNs, Nelson (2000) suggested that the stellar velocity dispersion of the host’s bulge can be estimated by assuming  $\sigma_* = \sigma_g$  ([O III]). Numerous studies have since adopted this strategy to investigate the  $M_{\text{BH}}\text{-}\sigma_*$  relation in AGNs (e.g., Wang & Lu 2001; Grupe & Mathur 2004) and its possible evolution with redshift (e.g., Shields et al. 2003; Salviander et al. 2007). However, the large observed scatter of the  $\sigma_g\text{-}\sigma_*$  correlation (Boroson 2003), not to mention the kinematic anomalies long known to afflict the [O III] line (Boroson 2005), gave cause for concern. To mitigate these uncertainties, Greene & Ho (2005a) recommended that only the core of the [O III] line be used, and, if possible, that [O III] be abandoned altogether in favor of lower-ionization transitions such as [O II]  $\lambda 3727$  or [S II]  $\lambda \lambda 6716, 6731$ .

This study shows that the width of [N II], another low-ionization line, also traces the stellar velocity dispersion of the bulge. The scatter is modest,  $\sim 0.2$  dex, but not insignificant. Since  $M_{\text{BH}} \propto \sigma_*^4$  (Tremaine et al. 2002), a 0.2 dex uncertainty on  $\sigma_*$  translates into a 0.8 dex (or factor of  $\sim 6$ ) uncertainty on  $M_{\text{BH}}$ . Importantly, we find that the velocity dispersion of the ionized gas does not identically match the velocity dispersion of the stars, but rather, on average,  $\sigma_g/\sigma_* \approx 0.8$ . Closer examination reveals that the residuals of the  $\sigma_g\text{-}\sigma_*$  relation in fact depend on AGN properties. The principal “second parameter” appears to be either the Eddington ratio ( $L_{\text{bol}}/L_{\text{Edd}}$ ) or some measure of the AGN luminosity (we use  $L_{\text{H}\alpha}$ ). The residuals seem to correlate somewhat better with  $L_{\text{bol}}/L_{\text{Edd}}$  than with  $L_{\text{H}\alpha}$ , although from our data alone we cannot truly tell which variable is more fundamental. Since the optical NLR luminosity correlates strongly with radio continuum luminosity (e.g., Ho & Peng 2001; Ulvestad & Ho 2001; Nagar et al. 2005), it is hardly surprising that  $\Delta\sigma$  correlates with radio power too, although the scatter is larger and the statistical significance is inferior compared to either  $L_{\text{H}\alpha}$  or  $L_{\text{bol}}/L_{\text{Edd}}$ . The dependence of the residuals of the  $\sigma_g\text{-}\sigma_*$  relation on  $L_{\text{bol}}/L_{\text{Edd}}$  was first noticed by Greene & Ho (2005a; later confirmed by Bian et al. 2006) for a large sample of more luminous AGNs selected from SDSS, and, within the uncertainties, the Palomar sources seem to follow roughly the low-luminosity extrapolation of the SDSS sample (Fig. 5). Curiously, Greene & Ho did not see any correlation between  $\Delta\sigma$  and AGN optical ([O III]) luminosity or radio power. It is possible that the large linear scales probed by SDSS (the 3'' fibers correspond to 5.4 kpc at  $z = 0.1$ ) introduce substantial uncertainties into measurements of the bulge and NLR.

The dependence of  $\Delta\sigma$  on AGN properties can be exploited to sharpen the  $\sigma_g\text{-}\sigma_*$  correlation as a tool to predict  $\sigma_*$  when the latter is, as is often the case, difficult or impractical to measure directly in AGNs. Even when a low-ionization line or only the core of the [O III] line is being used, as recommended by

Greene & Ho (2005a), it is important to realize that  $\sigma_g/\sigma_*$  is *not* identically equal to unity. Rather,  $\sigma_g/\sigma_*$  varies from  $\sim 0.6$  to  $\sim 1.4$  as a function of luminosity or Eddington ratio. Equations (1) and/or (3) should be used to obtain a more refined estimate of  $\sigma_*$ . Moreover, significant scatter still remains ( $\sim 0.15$  dex), even after correcting for the second parameter, most of which may be intrinsic and irreducible owing to the complexities of the NLR (Rice et al. 2006).

#### 4.2. Evidence for AGN Feedback

From a physical point of view, what is the origin of the  $\Delta\sigma$ - $L_{H\alpha}$  or  $\Delta\sigma$ - $L_{bol}/L_{Edd}$  correlations? As discussed further below, if the gas derives principally from mass loss from bulge stars, its kinematics should generally track the kinematics of the stars. But because the gas is collisional and experiences hydrodynamical drag against the surrounding hot medium, we expect it to be kinematically slightly colder than the stars. In the absence of additional energy input from other sources, we anticipate  $\sigma_g/\sigma_* \lesssim 1$ , as observed. As additional energy is injected into the system, for example from activation of the central black hole, the gas gains energy, to the point that  $\sigma_g$  approaches or even overtakes  $\sigma_*$ . Precisely how this is accomplished is unclear. Do AGNs impart mostly mechanical energy from outflows/winds or more highly collimated fast jets? Does radiation pressure matter? The empirical trends presented in this paper offer some insights into these issues, which ultimately have bearing on current interests in AGN feedback in galaxies.

The fact that the emission-line widths become systematically broader with increasing AGN activity—whatever the principal source of energy—implies that the gas is primarily accelerated rather than directly heated. The  $H\alpha$  luminosity, and presumably also the bolometric luminosity, strongly correlates with  $\Delta\sigma$ , but it seems doubtful that the radiation density itself plays a central role because H II nuclei with the same range in luminosity and sampled over a similar volume do not show the same effect. Compared to nuclear star formation, AGNs have a characteristically harder ionizing spectrum and a more centrally concentrated radiation field. Whether these factors result in more efficient radiative acceleration of the ionized gas in AGNs needs to be further investigated.

The radio-emitting plasma is an obvious suspect—that is, a scaled-down, but qualitatively similar agent as that responsible for super-virial acceleration in the most extreme, jet-dominated sources. This is a tenable hypothesis because nearly all Seyferts (e.g., Kukula et al. 1995; Ho & Ulvestad 2001; Ulvestad & Ho 2001) and LINERs (Nagar et al. 2005) and a sizable fraction of transition objects (Filho et al. 2000, 2002) contain nuclear radio sources, many with morphological structures resembling jets. The radio luminosity function of low-luminosity AGNs varies continuously over at least 4 orders of magnitude in radio power, from  $P_{20\text{cm}} \approx 10^{19}$  to  $10^{23}$  W Hz<sup>-1</sup> (Ulvestad & Ho 2001; Filho et al. 2006). There is no characteristic power that might demarcate a luminosity threshold above which radio sources become effective in perturbing the NLR. Although the degree of radio-loudness (expressed as the relative fraction of the radiative output emerging in the radio band) actually decreases with increasing Eddington ratio (Ho 2002; Terashima & Wilson 2003; Greene et al. 2006), Ho (2008) notes that extended, jetlike structures are more prevalent in high- $L_{bol}/L_{Edd}$  sources (Seyferts) than in low- $L_{bol}/L_{Edd}$  sources (LINERs). The radio cores in LINERs, despite being energetically more dominant, may be less effective at stirring up the NLR because

of their compact structure. The extended, linear features in Seyferts, on the other hand, can impact a larger pool of the circumnuclear material. Jet-induced interactions have been invoked to explain the morphology and kinematics of the NLR in a number of well-studied Seyfert galaxies (e.g., Mrk 78: Whittle & Wilson 2004; NGC 1068: Das et al. 2006; NGC 4151: Mundell et al. 2003). Despite the natural appeal of radio jets, however, our analysis shows that radio power correlates more poorly with  $\Delta\sigma$  than  $H\alpha$  luminosity or Eddington ratio.

We speculate that the dominant source of energy input comes from accretion disk winds, a common feature in AGNs (Crenshaw et al. 2003). Disk winds or outflows presumably agitate the NLR through shocks, provided that they do not violate other constraints that limit the role of shocks in the excitation of the gas (Ho 2008). The ability of an accretion disk to generate a wind may depend critically on  $L_{bol}/L_{Edd}$  (Proga 2007), and systems such as LINERs with ultra-low  $L_{bol}/L_{Edd}$  seem to lack outflows altogether (Ho 2008). Consistent with Greene & Ho (2005a), we propose that the Eddington ratio primarily accounts for the secondary line broadening in the NLR. The apparent interchangeability between  $L_{bol}/L_{Edd}$  and  $L_{H\alpha}$  is probably an artifact of the small dynamic range in black hole mass for the majority of the Palomar sample, coupled with the sizable intrinsic scatter in the  $\sigma_g$ - $\sigma_*$  relation.

#### 4.3. Line Width-Luminosity Correlation in AGNs

Phillips et al. (1983) first noticed that the luminosity of the [O III] line in Seyfert galaxies loosely correlates with its line width. This result has since been extended to much larger samples of Seyferts by Whittle (1985, 1992b) and Gu et al. (2006), as well as to lower-luminosity AGNs in the Palomar survey by Ho et al. (2003; using  $H\alpha$  for line luminosity and [N II] for line width). The form of the correlation is  $L_{NLR} \propto \text{FWHM}^a$ , where, depending on the study and sample, the slope can take a wide range of values, from  $a \approx 3$  to 6, with a typical value of  $\sim 4$ . The physical origin of the line width-luminosity relation has been unclear. Whittle (1992b) suggests that the line width-luminosity relation is actually a secondary correlation, reflecting on the one hand the more primary link between bulge mass and NLR velocity, and on the other various possible interdependencies among bulge mass, NLR luminosity, radio power, and line width.

In light of the results of this study and other recent developments, we offer a simple explanation. We have confirmed, as has long been suspected, that the widths of the narrow emission lines largely reflect the gravitational potential of the bulge, such that  $\text{FWHM} \propto \sigma_*$ . The bulge, meanwhile, directly links to the mass of the central black hole via the fundamental relation  $M_{BH} \propto \sigma_*^4$  (Tremaine et al. 2002). Now, a given  $M_{BH}$  radiates up its Eddington luminosity, which in turn is related to the NLR luminosity by a bolometric correction and the Eddington ratio (accretion rate) of the system. Hence, AGNs should populate a distribution whose *upper envelope* follows a ridge line defined by  $L_{NLR} \propto \text{FWHM}^4$ . At a given FWHM,  $L_{NLR}$  has a maximum but no hard minimum (other than that dictated by detection sensitivity). Indeed, this is what is seen. Ho et al. (2003) presented the line width-luminosity correlation separately for each of the three classes of AGNs in the Palomar survey, and it is clear that the zero point of the correlation shifts with the average luminosity of each class.

#### 4.4. Source of the Gas and Its Dynamical Support

As discussed in Ho (2008, 2009), the gas that ultimately fuels AGNs in nearby galaxies can be readily supplied internally by mass loss from evolved stars (red giants and planetary nebulae) in the bulge. The same argument, the gist of which was already advanced by Minkowski & Osterbrock (1959) to explain the origin of nebular emission seen in ellipticals, can be extended to include the entire gas reservoir that makes up the NLR in low-luminosity AGNs. Assuming  $T_e = 10^4$  K,  $n_e = 100$  cm $^{-3}$ ,  $H\alpha/H\beta = 3.1$ , and an effective recombination rate for H $\alpha$  of  $\alpha_{H\alpha}^{\text{eff}} = 9.36 \times 10^{-24}$  cm $^3$  s $^{-1}$  (Osterbrock 1989),

$$M_{\text{NLR}} = 2.97 \times 10^3 \left( \frac{100 \text{ cm}^{-3}}{n_e} \right) \left( \frac{L_{H\alpha}}{10^{38} \text{ erg s}^{-1}} \right) M_{\odot}. \quad (4)$$

From the population statistics of the Palomar survey assembled in Ho et al. (2003), LINERs and transition objects have median  $L_{H\alpha} \approx 7 \times 10^{38}$  erg s $^{-1}$  and  $n_e \approx 200$  cm $^{-3}$ , and hence  $M_{\text{NLR}} \approx 1 \times 10^4 M_{\odot}$ . The corresponding values for Seyferts are  $L_{H\alpha} \approx 40 \times 10^{38}$  erg s $^{-1}$ ,  $n_e \approx 400$  cm $^{-3}$ , and  $M_{\text{NLR}} \approx 3 \times 10^4 M_{\odot}$ . Strictly speaking, these values only pertain to the central 200 pc  $\times$  400 pc region sampled by the spectroscopic aperture, but given the high degree of central concentration of the line-emitting gas (Ho 2008), they probably underestimate the integrated values for the entire NLR by no more than a factor of  $\sim 2$ . These mass estimates can be compared with the amount of material shed from evolved stars. For a Salpeter stellar initial mass function with a lower-mass cutoff of  $0.1 M_{\odot}$ , an upper-mass cutoff of  $100 M_{\odot}$ , solar metallicities, and an age of 15 Gyr (Padovani & Matteucci 1993),

$$\dot{M}_* \approx 3 \times 10^{-11} \left( \frac{L_*}{L_{\odot,V}} \right) M_{\odot} \text{ yr}^{-1}. \quad (5)$$

With a median Hubble type of Sa, the host galaxies of the Palomar AGNs have sizable bulges and correspondingly healthy gas supply rates. For a median bulge luminosity of  $M_B \approx -19.3$  mag (Ho et al. 2003) and  $B - V = 0.8$  mag (Fukugita et al. 1995),  $\dot{M}_* \approx 0.5 M_{\odot} \text{ yr}^{-1}$ . These values pertain to the entire bulge. Within the spectroscopic aperture the nuclear stellar continuum luminosities (Ho et al. 1997a) are approximately a factor of 10 lower than the integrated luminosities, which implies  $\dot{M}_* \approx 0.05 M_{\odot} \text{ yr}^{-1}$ . Thus, stellar mass loss can sustain the gas reservoir in the NLR if the stellar debris survives for periods longer than  $\sim 2 \times 10^5 - 10^6$  yr before it dissipates and merges with the surrounding hot interstellar medium (Mathews 1990; Parriott & Bregman 2008).

If the ionized gas is mainly produced internally through stellar mass loss in the bulge<sup>4</sup>, what is the expected kinematical signature of this material? The supersonic motion of the ejecta through the ambient medium generates a strong shock that thermalizes the gas to the kinetic temperature of the stars,  $\sim 10^6 - 10^7$  K, on a timescale of  $\sim 10^5 - 10^6$  yr (Sanders 1981; Mathews 1990). Not all of the gas gets heated, however. Numerical simulations of mass loss from evolved stars in elliptical galaxies, after accounting for radiative cooling, predict that some fraction of the gas, perhaps  $\sim 20\%$ , remains cool (Parriott & Bregman 2008). Photoionization of this residual gas, as well

as the fresh ejecta prior to thermalization, produces the nebular emission visible in the optical.<sup>5</sup> During the early stages of their evolution, the mass loss envelopes orbit roughly cospatially with their parent stars and thus closely track their natal velocities. As bulge stars do not have a strong rotational component to their velocities, neither should the gas shed by them. After normalizing the gas line widths by the observed (projected) rotational velocity of the large-scale (HI) disk (Fig. 6), the significant, positive trend with galaxy inclination angle that remains implies that the ionized gas does not reside in a plane aligned with the large-scale galaxy. Moreover, the ejecta quickly lose memory of their birth sites as the material experiences drag deceleration against the surrounding hot medium. As discussed by Mathews (1990), the warm, optical-emitting clouds cannot be self-gravitating. Instead, they must be pressure-confined by the ambient hot medium, and hence their kinematics will largely imprint the local velocity of the hot gas. Since the hot gas is in virial equilibrium with the bulge stars, to first order we anticipate  $\sigma_g \approx \sigma_*$ . In detail, our analysis finds  $\sigma_g \approx 0.8\sigma_*$ . As the referee points out, supersonic turbulence in the hot gas rapidly dissipates through shocks. It is thus natural for  $\sigma_g$  to be slightly subvirial because the turbulence—the source of the random motions—is subsonic. When an AGN is present, the hot gas may be more agitated.

The scenario presented above provides a useful framework for interpreting a number of trends gleaned from spatially resolved observations of the central regions of galaxies. *Hubble Space Telescope* images frequently reveal dust lanes, spiral patterns, and a variety of other small-scale fine features in galaxy centers, but rarely do the structures ever take the form of thin, well-defined disks (Phillips et al. 1996; Carollo et al. 1997; Malkan et al. 1998; Pogge et al. 2000; Ho et al. 2002; Martini et al. 2003; Simões Lopes et al. 2007). Since the dust generally traces the nebular gas (e.g., Ravindranath et al. 2001; Falcón-Barroso et al. 2006), we can infer that the ionized gas more or less follows the same topology as the dust. The complex morphology of the gas strongly hints that its velocity field must be similarly chaotic. Where available, observations support this picture. For example, a number of authors have noted that the central rotation curves of the ionized gas often rise more slowly than the circular velocities predicted from the luminosity profile of the stars (Caldwell 1984; Caldwell et al. 1986; Fillmore et al. 1986; Kent 1988; Kormendy & Westpfahl 1989; Cinzano & van der Marel 1994; Bertola et al. 1995; Fisher 1997; Cinzano et al. 1999; Pignatelli et al. 2001), suggesting that random motions contribute appreciably to the dynamical support of the gas. On scales probed by the *Hubble Space Telescope*, very few objects exhibit clean signatures of dynamically cold disks undergoing circular rotation (Sarzi et al. 2001; Ho et al. 2002; Atkinson et al. 2005; Noel-Storr et al. 2007). Although the statistics are still quite limited, evidence is emerging that the degree of kinematic disturbance may be directly linked to the level of AGN activity (Verdoes Kleijn et al. 2006; Dumas et al. 2007; Walsh et al. 2008; § 4.2).

We end with the following note. The above discussion presupposes that the optical line emission comes exclusively from

<sup>4</sup>We do not mean to suggest that external acquisition of gas does not take place. Indeed, an external origin has been invoked to explain the distribution of kinematic axis misalignments between the gas and stars (Bertola et al. 1992; Caon et al. 2000; Sarzi et al. 2006), as well as certain HI properties (Ho 2007), in early-type galaxies.

<sup>5</sup>The optical line emission in ellipticals and bulges in principle can be excited by a variety of mechanisms, including photoionization by young or old hot stars, photoionization by a central AGN, shocks, self-irradiation from cooling condensations, and even cosmic ray heating by the radio-emitting plasma. With the possible exception of the weakest emission-line objects, however, Ho (2008) argues that the majority of the low-luminosity AGNs in the Palomar survey—essentially all nearby galaxies with sizable bulges—are powered by nonstellar photoionization.

stellar ejecta prior to their being mixed into the hot phase. There may be another component. Once the ejecta become thermalized, the hot gas, at least in the inner cores of bulges, should cool and condense on a relatively short timescale. Recent *Chandra* and *XMM-Newton* observations of ellipticals and bulges show that the diffuse X-ray-emitting medium typically has temperatures of  $kT \approx 0.3 - 1$  keV and densities of  $n \approx 0.1 - 0.3 \text{ cm}^{-3}$  (see Ho 2009 and references therein). Assuming  $kT = 0.5$  keV and  $n = 0.1 \text{ cm}^{-3}$ , the cooling time is merely  $\sim 6 \times 10^7$  yr. This simple picture of galactic-scale cooling flows encounters a number of long-standing difficulties familiar in the context of galaxy clusters, and their resolution appeals to similar remedies (Mathews & Brighenti 2003). A key ingredient to counter the overcooling problem invokes some form of energy feedback. It is tempting to associate the evidence for AGN feedback discussed in this paper (§ 4.2) with such a mechanism. The kinematics that ensue from the cooling flow scenario are likely to be quite complicated, but in general we also expect the cooling condensations to be in pressure balance with the surrounding hot medium and hence to reflect its kinematics. Depending on the shape of the potential, the cooling flow filaments can settle in different planes at different radii (Tohline et al. 1982). This may account for the variety of dust structures often seen in the central regions of early-type galaxies (e.g., Lauer et al. 2005).

#### 5. SUMMARY

We use a new catalog of stellar velocity dispersions to study the relationship between the kinematics of the ionized gas and the stars in the central few hundred parsecs of a large sample of nearby galaxies. The gas dispersions are based on the width of the [N II]  $\lambda 6583$  line. Robust measurements of both  $\sigma_g$  and  $\sigma_*$  are available for 345 galaxies spanning a wide range in Hubble type and level of nuclear activity. The principal results of our analysis can be summarized as follows.

1. The velocity dispersion of the ionized gas strongly correlates with, and is roughly comparable to, the velocity dispersion of the stars over the velocity range  $\sim 30 - 350 \text{ km s}^{-1}$ , across all Hubble types. This confirms the notion that the widths of the narrow emission lines primarily reflect the virial velocity of the gravitational potential of the stellar bulge. In detail,  $\sigma_g/\sigma_*$  ranges from  $\sim 0.6$  to 1.4, with an average value of 0.80.
2. The ratio  $\sigma_g/\sigma_*$  shows no strong dependence on Hubble type, for galaxies ranging from E to Sbc. Among galaxies of type Sc and later, systems with  $\sigma_* \lesssim 40 \text{ km s}^{-1}$ ,

all spectroscopically classified as H II nuclei,  $\sigma_g/\sigma_* \gtrsim 1$ . The ionized gas maintains a minimum “floor” dispersion of  $\sigma_g \approx 30 \text{ km s}^{-1}$ , which might signify a lower threshold level of interstellar turbulence generated by energy feedback from massive stars. The  $\sigma_g - \sigma_*$  relation does not depend on the presence of a large-scale bar or on the local environment of the galaxy.

3. The residuals of the  $\sigma_g - \sigma_*$  relation for AGNs (Seyferts, LINERs, and transition objects) correlate strongly with the nuclear optical (H $\alpha$ ) luminosity, and perhaps even stronger with the Eddington ratio. Radio power plays a less essential role. We argue that energy injected by accretion disk winds or outflows, not radio jets, provide a source of AGN feedback that accelerates the NLR gas to speeds above the virial velocities of the stars.
4. We confirm that the line widths of narrow emission lines can be used to obtain reasonably reliable estimates of  $\sigma_*$ , but, for maximum accuracy, preference should be given to low-ionization transitions such as [N II] and care should be taken to correct for the secondary dependence of  $\sigma_g$  on AGN luminosity or Eddington ratio.
5. We show that the mass budget of the ionized gas can be accounted for by mass loss from evolved stars. The optical line emission arises from photoionization of the just-shed, mass loss envelopes prior to their being thermalized, in conjunction with an additional contribution from filaments recondensing from the hot medium. We argue that the line widths are dominated by random motions, reflecting the kinematics of the hot gas that pressure confines the line-emitting clouds.
6. Lastly, we suggest that the line width-luminosity correlation in AGNs actually defines the upper envelope of a distribution of points governed by the  $\sigma_g - \sigma_*$  relation, the  $M_{\text{BH}} - \sigma_*$  relation, and the Eddington limit.

I am grateful to Joel Bregman, Jenny Greene, Janice Lee, and Mark Whittle for helpful correspondence. I thank Bill Mathews, the referee, for constructive criticisms that helped to clarify the discussion in §4.4. This work was supported by the Carnegie Institution of Washington and by NASA grants from the Space Telescope Science Institute, which is operated by the Association of Universities for Research in Astronomy, Inc., for NASA, under contract NAS5-26555.

#### REFERENCES

- Atkinson, J. W., et al. 2005, *MNRAS*, 359, 504  
 Baum, S. A., & McCarthy, P. J. 2000, *AJ*, 119, 2634  
 Bertola, F., Buson, L. M., & Zeilinger, W. W. 1992, *ApJ*, 401, L79  
 Bertola, F., Cinzano, P., Corsini, E. M., Rix, H.-W., & Zeilinger, W. W. 1995, *ApJ*, 448, L13  
 Bian, W., Gu, Q., Zhao, Y., Chao, L., & Cui, Q. 2006, *MNRAS*, 372, 876  
 Boroson, T. A. 2003, *ApJ*, 585, 647  
 ——. 2005, *AJ*, 130, 381  
 Botte, V., Ciroi, S., Di Mille, F., Rafanelli, P., & Romano, A. 2005, *MNRAS*, 356, 789  
 Busko, I. C., & Steiner, J. E. 1992, *MNRAS*, 258, 306  
 Caldwell, N. 1984, *PASP*, 96, 287  
 Caldwell, N., Kirshner, R. P., & Richstone, D. O. 1986, *ApJ*, 305, 136  
 Caon, N., Macchetto, D., & Pastoriza, M. 2000, *ApJS*, 127, 39  
 Carollo, C. M., Stiavelli, M., de Zeeuw, P. T., & Mack, J. 1997, *AJ*, 114, 2366  
 Chen, X.-Y., Hao, C.-N., & Wang, J. 2008, *ChJAA*, 8, 25  
 Cinzano, P., Rix, H.-W., Sarzi, M., Corsini, E. M., Zeilinger, W. W., & Bertola, F. 1999, *MNRAS*, 307, 433  
 Cinzano, P., & van der Marel, R. P. 1994, *MNRAS*, 270, 325  
 Crenshaw, D. M., Kraemer, S. B., & George, I. M. 2003, *ARA&A*, 41, 117  
 Das, V., Crenshaw, D. M., Deo, R. P., & Kraemer, S. B. 2006, *AJ*, 132, 620  
 Dasyra, K. M., et al. 2008, *ApJ*, 674, L9  
 Demoulin-Ulrich, M.-H., Butcher, H. R., Boksenberg, A. 1984, *ApJ*, 285, 527  
 de Vaucouleurs, G., de Vaucouleurs, A., Corwin, H. G., Jr., Buta, R. J., Paturel, G., & Fouqué, R. 1991, *Third Reference Catalogue of Bright Galaxies* (New York: Springer)  
 Dumas, G., Mundell, C. G., Emsellem, E., & Nagar, N. M. 2007, *MNRAS*, 379, 1249  
 Falcón-Barroso, J., et al. 2006, *MNRAS*, 369, 529  
 Ferrarese, L., & Merritt, D. 2000, *ApJ*, 539, L9  
 Filho, M. E., Barthel, P. D., & Ho, L. C. 2000, *ApJS*, 129, 93  
 ——. 2002, *ApJS*, 142, 223  
 ——. 2006, *A&A*, 451, 71

- Fillmore, J. A., Boroson, T. A., & Dressler, A. 1986, *ApJ*, 302, 208
- Fisher, D. 1997, *AJ*, 113, 950
- Fukugita, M., Shimasaku, K., & Ichikawa, T. 1995, *PASP*, 107, 945
- Gaskell, C. M., & Ferland, G. J. 1984, *PASP*, 96, 393
- Gebhardt, K., et al. 2000, *ApJ*, 539, L13
- Greene, J. E., & Ho, L. C. 2005a, *ApJ*, 627, 721
- . 2005b, *ApJ*, 630, 122
- . 2006, *ApJ*, 641, 117
- . 2007, *ApJ*, 667, 131
- Greene, J. E., Ho, L. C., & Ulvestad, J. S. 2006, *ApJ*, 636, 56
- Grupe, D., & Mathur, S. 2004, *ApJ*, 606, L41
- Gu, Q. S., Melnick, J., Cid Fernandes, R., Kunth, D., Terlevich, E., & Terlevich, R. 2006, *MNRAS*, 366, 480
- Heckman, T. M., Blitz, L., Wilson, A. S., Armus, L., & Miley, G. K. 1989, *ApJ*, 342, 735
- Heckman, T. M., Illingworth, G. D., Miley, G. K., & van Breugel, W. J. M. 1985, *ApJ*, 299, 41
- Heckman, T. M., Miley, G. K., van Breugel, W. J. M., & Butcher, H. R. 1981, *ApJ*, 247, 403
- Ho, L. C. 1996, in *The Physics of LINERs in View of Recent Observations*, ed. M. Eracleous et al. (San Francisco: ASP), 103
- . 2002, *ApJ*, 564, 120
- . 2007, *ApJ*, 668, 94
- . 2008, *ARA&A*, 46, 475
- . 2009, *ApJ*, in press
- Ho, L. C., Filippenko, A. V., & Sargent, W. L. W. 1995, *ApJS*, 98, 477
- . 1997a, *ApJS*, 112, 315
- . 1997b, *ApJ*, 487, 568
- . 1997c, *ApJ*, 487, 579
- . 2003, *ApJ*, 583, 159
- Ho, L. C., Filippenko, A. V., Sargent, W. L. W., & Peng, C. Y. 1997d, *ApJS*, 112, 391
- Ho, L. C., Greene, J. E., Filippenko, A. V., & Sargent, W. L. W. 2009, *ApJS*, in press
- Ho, L. C., & Peng, C. Y. 2001, *ApJ*, 555, 650
- Ho, L. C., Sarzi, M., Rix, H.-W., Shields, J. C., Rudnick, G., Filippenko, A. V., & Barth, A. J. 2002, *PASP*, 114, 137
- Ho, L. C., & Ulvestad, J. S. 2001, *ApJS*, 133, 77
- Isobe, T., Feigelson, E. D., & Nelson, P. I. 1986, *ApJ*, 306, 490
- Jiménez-Benito, L., Díaz, A. I., Terlevich, R., & Terlevich, E. 2000, *MNRAS*, 317, 907
- Kent, S. M. 1988, *AJ*, 96, 514
- Kormendy, J., & Kennicutt, R. C. 2004, *ARA&A*, 42, 603
- Kormendy, J., & Westpfahl, D. J. 1989, *ApJ*, 338, 752
- Kukula, M. J., Pedlar, A., Baum, S. A., O’Dea, C. P. 1995, *MNRAS*, 276, 1262
- Kuzio de Naray, R., McGaugh, S. S., & de Blok, W. J. G. 2008, *ApJ*, 676, 920
- Laor, A. 2003, *ApJ*, 590, 86
- Lauer, T. R., et al. 2005, *AJ*, 129, 2138
- Malkan, M. A., Gorjian, V., & Tam, R. 1998, *ApJS*, 117, 25
- Martini, P., Regan, M. W., Mulchaey, J. S., & Pogge, R. W. 2003, *ApJ*, 589, 774
- Mathews, W. G. 1990, *ApJ*, 354, 468
- Mathews, W. G., & Brighenti, F. 2003, *ARA&A*, 41, 191
- Minkowski, R., & Osterbrock, D. E. 1959, *ApJ*, 129, 583
- Mundell, C. G., Wrobel, J. M., Pedlar, A., & Gallimore, J. F. 2003, *ApJ*, 583, 192
- Nagar, N. M., Falcke, H., & Wilson, A. S. 2005, *A&A*, 435, 521
- Nelson, C. H. 2000, *ApJ*, 544, L91
- Nelson, C. H., & Whittle, M. 1995, *ApJS*, 99, 67
- . 1996, *ApJ*, 465, 96
- Noel-Storr, J., Baum, S. A., & O’Dea, C. P. 2007, *ApJ*, 663, 71
- Osterbrock, D. E. 1989, *Astrophysics of Gaseous Nebulae and Active Galactic Nuclei* (Mill Valley: Univ. Science Books)
- Padovani, P., & Matteucci, F. 1993, *ApJ*, 416, 26
- Parriott, J. R., & Bregman, J. N. 2008, *ApJ*, 681, 1215
- Phillips, A. C., Illingworth, G. D., MacKenty, J. W., & Franx, M. 1996, *AJ*, 111, 1566
- Phillips, M. M., Charles, P. A., & Baldwin, J. A. 1983, *ApJ*, 266, 485
- Phillips, M. M., Jenkins, C. R., Dopita, M. A., Sadler, E. M., & Binette, L. 1986, *AJ*, 91, 1062
- Pignatelli, E., et al. 2001, *MNRAS*, 323, 188
- Pizzella, A., Corsini, E., Sarzi, M., Magorrian, J., Mendez-Abreu, J., Coccato, L., & Bertola, F. 2008a, *MNRAS*, 387, 1099
- Pizzella, A., Tamburro, D., Corsini, E. M., & Bertola, F. 2008b, *A&A*, 482, 53
- Pogge, R. W., Maoz, D., Ho, L. C., & Eracleous, M. 2000, *ApJ*, 532, 323
- Proga, D. 2007, in *The Central Engine of Active Galactic Nuclei*, ed. L. C. Ho & J.-M. Wang (San Francisco: ASP), 267
- Ravindranath, S., Ho, L. C., Peng, C. Y., Filippenko, A. V., & Sargent, W. L. W. 2001, *AJ*, 122, 653
- Rice, M. S., Martini, P., Greene, J. E., Pogge, R. W., Shields, J. C., Mulchaey, J. S., & Regan, M. W. 2006, *ApJ*, 636, 654
- Salviander, S., Shields, G. A., Gebhardt, K., & Bonning, E. W. 2007, *ApJ*, 662, 131
- Sanders, R. H. 1981, *ApJ*, 244, 82
- Sarzi, M., et al. 2006, *MNRAS*, 366, 1151
- Sarzi, M., Rix, H.-W., Shields, J. C., Rudnick, G., Ho, L. C., McIntosh, D. H., Filippenko, A. V., & Sargent, W. L. W. 2001, *ApJ*, 550, 65
- Schmitt, J. H. M. M. 1985, *ApJ*, 293, 178
- Shields, G. A., Gebhardt, K., Salviander, S., Wills, B. J., Xie, B., Brotherton, M. S., Yuan, J., & Dietrich, M. 2003, *ApJ*, 583, 124
- Simões Lopes, R. D., Storchi-Bergmann, T., de Fátima de O. Saraiva, M., & Martini, P. 2007, *ApJ*, 655, 718
- Smith, E. P., Heckman, T. M., & Illingworth, G. D. 1990, *ApJ*, 356, 399
- Terashima, Y., & Wilson, A. S. 2003, *ApJ*, 583, 145
- Terlevich, E., Díaz, A. I., & Terlevich, R. 1990, *MNRAS*, 242, 271
- Tohline, J. E., Simonson, G. F., & Caldwell, N. 1982, *ApJ*, 252, 92
- Tremaine, S., et al. 2002, *ApJ*, 574, 740
- Ulvestad, J. S., & Ho, L. C. 2001, *ApJ*, 558, 561
- Vega Beltrán, J. C., Pizzella, A., Corsini, E. M., Funes, J. G., Zeilinger, W. W., Beckman, J. E., & Bertola, F. 2001, *A&A*, 374, 394
- Veilleux, S. 1991, *ApJS*, 75, 383
- Verdoes Kleijn, G. A., van der Marel, R. P., & Noel-Storr, J. 2006, *AJ*, 131, 1961
- Véron, M.-P. 1981, *A&A*, 100, 12
- Vrtilek, J. M., & Carleton, N. P. 1985, *ApJ*, 294, 106
- Walsh, J. L., Barth, A. J., Ho, L. C., Filippenko, A. V., Rix, H.-W., Shields, J. C., Sarzi, M., & Sargent, W. L. W. 2008, *AJ*, 136, 1677
- Wang, T.-G., & Lu, Y.-J. 2001, *A&A*, 377, 52
- Whittle, M. 1985, *MNRAS*, 213, 1
- . 1992a, *ApJS*, 79, 49
- . 1992b, *ApJ*, 387, 109
- . 1992c, *ApJ*, 387, 121
- . 1993, in *The Nearest Active Galaxies*, ed. J. Beckman, L. Colina, & H. Netzer (Madrid: CSIC Press), 63
- Whittle, M., & Wilson, A. S. 2004, *AJ*, 127, 606
- Wilson, A. S., & Heckman, T. M. 1985, in *Astrophysics of Active Galaxies and Quasi-Stellar Objects*, ed. J. S. Miller (Mill Valley, CA: Univ. Science Books), 39
- Zhou, H.-Y., Wang, T.-G., Yuan, W., Lu, H., Dong, X., Wang, J., & Lu, Y. 2006, *ApJS*, 166, 128